HHS Public Access

Author manuscript

Nat Methods. Author manuscript; available in PMC 2015 June 01.

Published in final edited form as:

Nat Methods. 2014 December ; 11(12): 1245–1252. doi:10.1038/nmeth.3151.

Cell-based reporters reveal *in vivo* dynamics of dopamine and norepinephrine release in murine cortex

Arnaud Muller[1,*], **Victory Joseph**[4,*], **Paul A. Slesinger**[4,5], and **David Kleinfeld**[1,2,3,4]

[1]Department of Physics, University of California at San Diego, La Jolla, CA

[2]Section of Neurobiology, University of California at San Diego, La Jolla, CA

[3]Department of Electrical & Computer Engineering, University of California at San Diego, La Jolla, CA

[4]Graduate Program in Neurosciences, University of California at San Diego, La Jolla, CA

[5]Dept. of Neuroscience, Icahn School of Medicine at Mount Sinai, New York, NY

Abstract

Neuronal coding of stimulus-to-action sequences are believed to involve the release of dopamine (DA) and norepinephrine (NE). The electrochemical similarity of these monoamines, however, confounds real-time measurements of their release. Here we report the creation of cell-based neurotransmitter fluorescent-engineered reporters (CNiFERs) that utilize the specificity of G-protein coupled receptors (GPCRs) to discriminate nanomolar concentrations of DA and NE. CNiFERs were implanted into frontal cortex of mice to measure the timing of neurotransmitter release during classical conditioning using two-photon microscopy. The onset of DA release correlated with that of licking and monotonically shifted from the time of the reward toward that of the cue. In contrast, concurrent release of NE did not correlate with licking or the cue. This new generation of CNiFERs provides unique tools to assess the release of monoamines. The molecular design of these CNiFERs may be generalized to realize CNiFERs for any molecule that activates a GPCR.

Keywords

Biophotonics; imaging; implantable sensors; learning; monoamines; two-photon microscopy

Corresponding authors: David Kleinfeld, dk@physics.ucsd.edu. Paul Slesinger, paul.slesinger@mssm.edu. Editorial correspondence: David Kleinfeld, Department of Physics 0374, University of California, 9500 Gilman Drive, La Jolla, CA 92093-0374, Phone – 858-822-0342, dk@physics.ucsd.edu.

*Equal contribution

AUTHOR CONTRIBUTIONS

All authors contributed to the experimental design and realization, analysis of the data, and writing of the paper. A. M. and V. J. performed the *in vitro* testing and *in vivo* imaging and behavioral experiments. D. K. and P. A. S. dealt with the myriad of university organizations that govern animal health and welfare, surgical procedures, and laboratory health and safety issues that include specific oversight of chemicals, controlled substances, human cell lines, lasers, and viruses.

COMPETING FINANCIAL INTERESTS

All authors declare no financial interests in this work.

INTRODUCTION

Neuronal processing in cortex plays an essential role in the transformation of sensory perception into motor actions. Neurotransmitters, which signal via slow extra-synaptic pathways as well fast synaptic pathways, are involved in the plasticity and refinement of neuronal processing that underlies the execution of behaviors. Slow signaling occurs through volume transmission over a period of seconds, as opposed to the millisecond scale for fast synaptic transmission[1,2]. The transmitters involved in slow signaling are believed to drive the plasticity of neural circuits and network activity. In particular, the monoamines dopamine (DA) and norepinephrine (NE) are required for the brain to adapt to a changing environment, such as in the formation of working memories, changes in attention, enhancement of decision-making[3–5], and perceptual learning[6,7]. A major obstacle in neuroscience has been the inability to detect the release of DA and NE *in vivo* with sufficient chemical specificity, spatial resolution, and temporal resolution.

Primarily two techniques have been established to measure the extracellular concentration of neuromodulators *in vivo*. The most common technique is microdialysis[8]. A dialysis cannula is stereotaxically implanted into the brain and samples are collected for identification by high-performance liquid chromatography and electrochemical detection. While microdialysis can accurately identify neurotransmitters[9,10], it requires the collection of relatively large samples and has poor temporal resolution, exceeding ten minutes per sample in the case of monoamines[11]. Moreover, the insertion of microdialysis probes can disrupt monoaminergic activity near the probe track[12]. The second method to measure the extracellular concentration of neuromodulators is fast-scan cyclic voltammetry (FSCV). This technique improves on the temporal resolution, *i.e.*, ~ 100 ms as opposed to hundreds of seconds for microdialysis, spatial resolution, *i.e.*, ~ 100 μm as opposed to a few millimeters for a cannula, and has nanomolar sensitivity. The use of FSCV has been most successful for the detection of dopamine and serotonin, yet DA and NE, which differ by a single hydroxyl side-group, have indistinguishable cyclic voltammetry signatures when they oxidize on traditional carbon potentiometric probes[13]. Thus FSCV use has been limited to areas of the brain in which only one of DA or NE is thought to be present. For example, cyclic voltammetry is commonly used in the striatum, which receives a strong DA projection[14]. However, measuring DA and NE in neocortex, which receives strong projections from dopaminergic and noradrenergic neurons, has remained a formidable challenge for cyclic voltammetry.

To address the current limitations in measuring neurotransmitters *in vivo*, we have developed a new technology to optically detect the release of classical neurotransmitters in the brain. Previously, we created a cell-based neurotransmitter fluorescent engineered reporter (CNiFER) for detecting acetylcholine[15]. CNiFERs are implanted into target brain regions where they report changes in neurotransmitter release *in vivo*. Important advantages of CNiFERs are their detection of nanomolar, physiological concentrations of neurotransmitter combined with their temporal resolution of seconds and spatial resolution of less than 100 μm. These sensors are clonal cell-lines engineered to express a specific G_q-type G protein coupled receptor (GPCR) that triggers an increase in intracellular [Ca^{2+}] which, in turn, is rapidly detected by a genetically encoded FRET-based Ca^{2+} sensor. This

system transforms neurotransmitter receptor binding into a change in fluorescence and provides a direct and real-time optical readout of local neurotransmitter activity. Furthermore, by utilizing the natural receptor for a given transmitter, CNiFERs gain the chemical specificity and temporal dynamics present *in vivo*. By utilizing a strategy for redirecting $G_{i/o}$ coupled GPCRs to the phospholipase-C/inositol 1,4,5-trisphosphate (PLC/IP_3) pathway[16], we report here the creation of two new CNiFERs to detect DA and NE.

To test the function of monoamine CNiFERs *in vivo*, we simultaneously imaged DA- and NE-sensitive CNiFERs implanted in frontal cortex of mice as they learned to associate a cue with a reward during classical conditioning. Dopamine neurons in the midbrain transiently spike during reinforcement[17] and release DA in the striatum and cortex[2,18]. Previous studies demonstrated that classically conditioned cue-reward pairings increased neuronal firing in midbrain neurons with a temporal shift from the time of the reward, *i.e.*, the unconditioned stimulus, to the time of the predictive cue, *i.e.*, the conditioned stimulus[19]. Similarly, neurons in the locus coeruleus transiently spike in response to task-relevant stimuli[3,20], suggesting that NE levels may also increase in the cortex during conditioning. Dialysis studies have shown efflux of both DA and NE in the cortex during conditioning[11,18], but these measures lacked sufficient temporal resolution to determine the relationship of their release to specific stimuli and cognitive processes within conditioning trials. We use DA- and NE-sensitive CNiFERs to readdress these issues with real-time, concurrent measurements of DA and NE release in murine frontal cortex during behavioral conditioning.

RESULTS

Creation of CNiFERs to detect DA or NE

A CNiFER is derived from a HEK293 cell that is engineered to stably express at least two proteins: (*i*) a specific G-protein coupled receptor (GPCR) and (*ii*) TN-XXL, a genetically encoded [Ca^{2+}] sensor based on fluorescence resonance energy transfer (FRET) between cyan and yellow fluorescent proteins (CFP and YFP, respectively) that utilizes a component of troponin to bind Ca^{2+} ions[15,21]. Activation of GPCRs that couple to endogenous G_q G-proteins trigger an increase in cytosolic [Ca^{2+}] through the PLC/IP_3 pathway, leading to an increase in FRET from the TN-XXL (Fig. 1a,b). The increase in FRET provides a rapid optical read-out of the change in neurotransmitter levels. To develop a new CNiFER for detecting DA and one for NE, we selected two GPCRs with high affinity and selectivity; the D2 dopaminergic receptor and the α1a adrenergic receptor (Fig. 1a,b). The α1a adrenergic receptor couples to G_q G-proteins and could be introduced directly into HEK293 cells. The D2 dopaminergic receptor, on the other hand, couples to $G_{i/o}$ G-proteins and first required the creation of a clonal HEK293 line that expresses G_{qi5}, a chimeric G-protein[16]. This chimeric G-protein contains primarily the $G\alpha_q$ sequence but the five amino acids of the carboxyl terminus have been replaced with those of $G\alpha_{i/o}$ to enable coupling to the D2 receptor but signaling through the PLC/IP_3 pathway (Fig. 1a,b).

HEK293 cells were first transduced with replication deficient lentivirus to express the TN-XXL calcium indicator. Following FACS analysis, clonal cells were screened for the

greatest response to an increase in the internal calcium concentration. This clonal line, with only the calcium indicator, is denoted clone 3g8. To create the α1a-CNiFER, clone 3g8 was subsequently transduced with a lentivirus that expressed the α1a adrenergic receptor. To create the D2-CNiFER, clone 3g8 was transduced with a lentivirus that expressed the chimeric G_{qi5} protein, forming a G_{qi5}.-expressing clone denoted qi5.6, and transduced again with a lentivirus to stably express the D2 receptor.

To identify the CNiFER clones with the best sensitivity to the native ligand and smallest response to other neurotransmitters, we used a high-throughput fluorometric plate reader to screen the individual clonal lines. Two lines, D2-CNiFER (clone D2.2) and α1a-CNiFER (clone α1a.6) were selected for more detailed analyses. Importantly, the parent lines lacking the receptors, clones 3g8 and qi5.6, serve as control CNiFERs. An example of the FRET response from the plate reader shows that agonist application leads to a step-decrease of CFP emission and a step-increase of YFP emission (Fig. 1c). The calculated fractional change in fluorescence, ΔF/F, for each signal (Fig. 1c; **upper panel**) was used to obtain the FRET ratio, denoted ΔR/R (Fig. 1c; **lower panel**) (Methods).

In vitro characterization of D2- and α1a-CNiFERs

How sensitive and specific are the new CNiFERs to the chosen agonists? The D2-CNiFER displayed nanomolar sensitivity to DA, with an EC_{50} = 2.5 ± 0.1 nM (mean ± SEM, here and everywhere unless specified; n = 3 runs), and a response to NE that was ~ 30 times less sensitive than DA (EC_{50} = 81 ± 8 nM for NE) (Fig. 1d; **left panel**). Similarly, the α1a-CNiFER exhibited nanomolar sensitivity to NE with an EC_{50} = 19 ± 1 nM (n = 3) and a DA response at high concentrations (EC_{50} = 1.4 ± 0.1 μM for DA) (Fig. 1d; **right panel**). Importantly, the dynamic ranges of the D2-and α1a-CNiFERs are comparable to the levels of monoamines measured with microdialysis[11,22,23] and FSCV[24,25] in the rodent brain. As a control, we examined HEK293 lines lacking the GPCR. We observed that the G_{qi5}-TN-XXL HEK293 line (Fig. 1d; **left panel, dotted line;qi5.6**) and TN-XXL HEK293 line (Fig. 1d; **right panel, dotted line;3g8**) showed an insignificant FRET response to either DA or NE at high concentrations (n = 3 for each condition, p > 0.08).

To test for non-specific receptor activation, we conducted a full panel screen using a set of common neurotransmitters at a low (50 nM) and a high concentration (1 μM) (Fig. 1e). The D2-CNiFER did not show appreciable response to most agonists and only responded weakly to somatostatin (ΔR/R = 0.2), acetylcholine (ΔR/R = 0.1) and vasointestinal peptide (VIP) (ΔR/R = 0.1) at 1 μM. The α1a-CNiFER did not show appreciable response to other agonists.

We next investigated the pharmacological receptor specificity of the D2- and α1a-CNiFERs since HEK293 cells possess endogenous GPCRs (Fig. S1). The D2-CNiFER response to 20 nM DA was not significantly altered following pre-incubation with the D1 receptor antagonist SCH23390 (100 nM) (normalized ΔR/R = 1.00 ± 0.03, n = 5, p = 0.99, unpaired t-test), but was fully blocked by pre-incubation with the D2 receptor antagonist eticlopride (50 nM) (normalized ΔR/R = 0.04 ± 0.02, n = 5, p = 0.0003, unpaired t-test). Similarly, the response of the α1a-CNiFER to 50 nM NE was not significantly altered by pre-incubation with the β-adrenergic receptor antagonist sotatol (5 μM) (normalized ΔR/R = 0.82 ± 10, n =

4, p = 0.17, unpaired t-test) but was strongly suppressed by pre-incubation with the α1a-antagonist WB4101 (50 nM) (normalized ΔR/R = 0.09 ± 0.03, n = 4, p = 0.0001, unpaired t-test). Taken together, these data establish the specificity of the D2- and α1a-CNiFERs.

The natural release of both NE and DA *in vivo* can be pulsatile. It was thus important to determine the response of CNiFERs to a pulse of agonist. We used a fast perfusion system to apply pulses at near-saturating concentrations, *i.e.*, 2.5 s pulses of 100 nM agonist mixed with a fluorescent dye, as illustrated by the data of Figure 2a for the response of a cluster of CNiFERs to a single pulse. At the level of individual cells (n = 20), a D2-CNiFER responded with a delay of 2.9 ± 0.2 s, reached a maximum response at 6.9 ± 0.6 s after the pulse onset, and had a maximum FRET ratio of 0.57 ± 0.03 (± 0.13 SD for a cell-to-cell variability of 23 %) (Fig. S2a). Similarly, pulses of NE increased the FRET ratio for an individual α1a-CNiFER with a delay of 2.3 ± 0.1 s, reached a maximum at 5.1 ± 0.3 s, and had a FRET ratio of 0.90 ± 0.05 (± 0.22 SD for a cell-to-cell variability of 24 %) (Fig. S2b). At this agonist concentration, the FRET signal returned to baseline in ~ 20 s. Previous studies using FRET probes[26] and bioluminescence resonance energy transfer signals[27] suggest this recovery time can be accounted for by the intrinsic properties of the GPCR signaling pathway. These data show that individual CNiFERs exhibit a reliable, robust response to pulsatile changes in agonist concentration.

To determine how CNiFERs respond to repeated agonist stimulation and to assess the temporal resolution of the new CNiFERs, we used two 2.5 s pulses of agonist that were separated by a variable amount of time (Fig. 2b). Both D2- and α1a-CNiFERs FRET responses could be distinguished with an inter-stimulus interval of only 5 s. We also investigated possible receptor desensitization using a 60 s long pulse delivered every four minutes for 40 minutes (Fig. 2c). The D2-CNiFER response decreased slightly between the first and the second pulse of agonist, but remained stable thereafter (n = 3) (Fig. 2c; **left panel**). The α1a-CNiFER showed a consistent FRET ratio across pulses (n = 3) (Fig. 2c; **right panel**). Taken together, these experiments demonstrate that both the D2- and α1a-CNiFERs respond reliably with little attenuation in an environment of repeated neurotransmitter exposure.

In vivo characterization of D2- and α1a-CNiFERs

We first established that each CNiFER could detect endogenous release of neurotransmitters when injected into the rodent brain. The mesolimbic DA circuit involves two primary DA pathways; VTA DA neurons that project to ventral striatum (NAc) and mPFC, and SN DA neurons that project to dorsal striatum and broadly to cortical regions[28]. To confirm the presence of direct projections from both dopaminergic and noradrenergic nuclei to the frontal cortex, we injected a neuronal retrograde tracer, Fluorogold™, in the frontal cortex and searched for neurons co-labeled with Fluorogold™ and tyrosine hydroxylase, a biosynthetic enzyme for both DA and NE (Fig. S3a,b). Three-dimensional reconstructions revealed that the majority of dopaminergic projections to the frontal cortex originated from substantia nigra (SN) (95 ± 2 % of co-labeled neurons, n = 4) (Fig. S3c; **left panel**), confirming previous studies that have shown projections from the SN to the prefrontal and motor cortex in rat[28] and monkey[29,30]. We observed relatively few neurons co-labeled for

Fluorogold™ and tyrosine hydroxylase in the mouse ventral tegmental area (5 ± 2 % of co-labeled neurons), although such projections to frontal cortex have been reported[31]. Three-dimensional reconstruction also revealed that the noradrenergic inputs originated from the locus coeruleus (LC) (Fig. S3c; **right panel**), corroborating previous studies with monkey[32] and rat[33].

An advantage of implanting CNiFERs in the brain to monitor *in vivo* release of neurotransmitters is that repeated measurements can be made across multiple days of behavioral training and experimentation. We formed a polished and reinforced thinned-skull (PoRTS) window over the frontal cortex for transcranial imaging[34] and stereotaxically injected CNiFERs into mouse frontal cortex at discrete sites located 200 to 300 μm below the cortical surface, *i.e.*, layers 2/3 (Fig. 3a; **left panels**). To address the possibility that the surgical procedure or presence of human cells introduced damage or inflammation in the cortex, we prepared mice for histological assessment of inflammation 7 days after implantation of the CNiFERs. Immunostaining for glial fibrillary acidic protein (GFAP), a marker of inflammation, revealed a small increase in GFAP-positive cells in both injected and control mice, *i.e.*, animals with a window but no implanted cells (Fig. 3a). This indicates that the presence of CNiFER cells did not induce significant damage although formation of the PoRTS window led to potential inflammation. Critically, no glial scars were found around the CNiFERs one week after the implantation. To examine activated microglia, we immunostained for MAC1 and did not observe any detectable staining. This latter result is consistent with the claims that a thinned skull preparation does not induce an apparent inflammatory response[34]. Taken together, these histological experiments suggest there is minimal damage caused by the injection of HEK293 cells into the cortex of mice.

We examined if the D2- and α1a-CNiFERs could detect an induced release of DA or NE, respectively, in the chronic preparation. We formed a PoRTS window over the frontal cortex, implanted electrodes into either the SN or LC for electrical stimulation, and stereotaxically injected CNiFERs. Each *in vivo* two-photon imaging plane contained 5 to 20 CNiFERs. After a day of recovery from the surgery, a single burst of electrical stimulation in the SN led to an increase in the FRET ratio for the D2-CNiFER within 2 s of the stimulation. The amplitude of the FRET response varied with the amplitude of the stimulation, with 50 μA stimulation producing a $\Delta R/R = 0.04 \pm 0.01$ (mean ± SD, n = 4) and 300 μA stimulation eliciting a $\Delta R/R = 0.21 \pm 0.06$ (Fig. 3b). We next measured the effect of cocaine on the D2-CNiFER response upon electrical stimulation of the SN. As expected for a DA reuptake inhibitor, 15 mg/kg (i.p.) cocaine enhanced the size of the D2 CNiFER FRET response following 100 μA stimulation. The ΔR/R in response to the stimulation increased from 0.09 ± 0.02 before the cocaine injection to 0.24 ± 0.02 after the cocaine injection ($p < 0.01$, unpaired t-test, n = 3) (Fig. 3b; **blue trace**). The duration of the signal, measured from the onset of the response to the return to the baseline was also increase from 27 ± 4 s to 61 ± 7 s after the cocaine injection.

Like the D2-CNiFER, the α1a-CNiFER response increased following electrical stimulation of the LC (Fig. 3c, **n = 3**), with a $\Delta R/R = 0.07 \pm 0.02$ for 50 μA stimulation and $\Delta R/R = 0.24 \pm 0.06$ for 200 μA stimulation. Thus, both D2- and α1a-CNiFERs appear to exhibit a dynamic range *in vivo* suitable to measure release of DA and NE in behaving mice. We

confirmed the receptor-specificity of each CNiFER *in vivo* with systemic injection of receptor-specific antagonists which blocked CNiFER responses to electrical stimulation (Fig. 3b,c; **orange traces**) ($p < 0.001$, unpaired t-test, $n = 3$). In addition, control CNiFERs showed little response to electrical stimulation (Fig. 3b,c; **purple traces**) ($p < 0.001$, unpaired t-test, $n = 3$). The duration of the FRET response varied between 20 s with weak stimulation to more than a minute with strong stimulation (Fig. 3b,c; **left panels**), consistent with CNiFERs detecting volume transmission of neurotransmitters in the cortex.

We determined if D2- and α1a-CNiFERs maintain their sensitivity *in vivo*. CNiFERs were stereotaxically injected into mouse frontal cortex through a craniotomy and a micropipette was placed with a tip approximately 100 μm from the implant. We measured the *in vivo* response of a cluster of CNiFERs to a train of pulses of agonist delivered concurrent with a fluorescent indicator. The D2-CNiFER displayed an *in vivo* sensitivity to DA with an EC_{50} = 29 ± 5 nM (mean ± SEM, n = 4) (Fig. 4d; **left panel**) The α1a-CNiFER exhibited an *in vivo* sensitivity to NE with an EC_{50} = 90 ± 21 nM (n = 4) (Fig. 4d; **right panel**). An increase in the apparent *in vivo* values for EC_{50} compared with the *in vitro* values was expected from the dilution of agonist as it diffused from the pipet to the site of the implant[35]. We found a dilution of 0.16 ± 0.03 (mean ± SEM, n = 14), which explains half of the apparent increase in EC_{50} for D2-CNiFERs and all of the increase for α1a-CNiFERs compared to the *in vitro* results (Fig. 1d). The former difference could result from *in situ* effects of the brain environment on the sensitivity of the D2 GPCR.

Simultaneous measurement of neuromodulators during behavioral conditioning

Previous studies have revealed that classically conditioned cue-reward pairings increase neuronal firing in midbrain neurons, with a temporal shift from the time of the reward, *i.e.*, the unconditioned stimulus, to the time of the predictive cue, *i.e.*, the conditioned stimulus. Similarly, neurons in the locus coeruleus transiently spike in response to task-relevant stimuli[3,20], suggesting that NE levels may also increase in the cortex during conditioning. Using the new D2- and α1a-CNiFERs, we probed the timing of DA and NE release during learning using a basic Pavlovian conditioning paradigm in head-fixed mice.

We implemented a paradigm consisting of a 5 s tone, *i.e.*, the conditioned stimulus (CS) followed by a drop of 10 % sucrose solution, *i.e.*, the unconditioned stimulus (US), that was delivered 3 s after the end of the tone (Fig. 4a). Prior to training the mice, we injected them with D2-CNiFERs alone or with α1a-CNiFERs in discrete sites separated by ~ 300 μm, in layers 2/3 of frontal cortex (Fig. 4b). We then measured the FRET responses from the D2- and α1a-CNiFERs using two-photon microscopy and measured motor behavior with a lickometer while mice learned to associate the 5 s tone with delivery of the sucrose solution (Fig. 4c). Although the delivery of the reward was not dependent on the animal's behavior, the dropper was positioned just beyond the animal's mouth such that the animal was required to make a motor act, tongue protrusion and licking, in order to retrieve the drop of sucrose. We hypothesized that the release of DA in the frontal cortex would shift from the time of the reward to the time of the predictive cue (CS). In an additional cohort of mice, we implanted M1-CNiFERs[15] or the D2-CNiFERs in two distinct areas. We predicted

engagement of the cholinergic (ACh) system in frontal cortex when animals made an explicit movement[36], such as licking.

We detected an increase in the FRET ratio for both D2- and α1a-CNiFERs within a single trial of conditioning and with a high signal-to-noise ratio (single trace example in Fig. 4d). The D2- and α1a-CNiFERs responded on the majority of trials. Simultaneous measurements of the D2- and M1-CNiFER responses, and concomitant licking, were also observed on a single trial basis with a high signal-to-noise ratio during conditioning trials (single trace example in Fig. 4e). The transient increases in [DA] and [NE] were similar in duration, with a full-width at half maximum amplitude of 25 ± 1 s (mean ± SEM; 13 mice) and 28 ± 1 s (8 mice) for [DA] and [NE], respectively. In contrast, [ACh] transients to a burst of licks persisted for a shorter interval, *i.e.*, 15 ± 1 s (4 mice).

The onset time of licking across multiple days of training exhibited a monotonic shift from the time of the reward to that of the cue (single trace example in Fig. 4f). Quantitatively, we observed a statistically significant decrease in the time to lick, with a slope of −0.40 ± 0.14 s per day ($p = 0.05$; 13 mice) (Figs. 5a and S4a). These data confirmed that mice learned to associate the CS with the US. Are there changes in volume transmission of DA and NE that track the change in licking behavior? We observed a statistically significant decrease in the mean onset time of the FRET ratio with the D2-CNiFER. Collectively, the D2-CNIFER FRET onset shifted from 10.3 ± 0.6 s (mean ± SEM; 13 mice) during the first day of training to 5 ± 0.3 s during the last day of training with a slope of −1.1 ± 0.14 s per day ($p = 0.02$; 13 mice) (Figs. 5b and S4b). Thus the release of DA shifted monotonically from the time of the reward toward the time of the cue, similar to licking. In contrast with the D2-CNiFER response, the onset of the α1a-CNIFER FRET response did not show an appreciable change across conditioning days with a average delay of 10.8 ± 1.4 s during the first day of training and 9.7±1.1s during the last day of training ($p = 0.6$; 7 mice) (Figs. 5c and S4c). Notably, the timing of NE release was highly variable both within a set of trials for a given animal as well as across animals over conditioning days.

The release of ACh, unlike that of DA, remained closely linked to the time of presentation of the reward, as measured by the onset time of M1 CNiFER FRET responses across conditioning trials. The M1-CNiFER FRET onset shifted from 9.0 ± 0.6 s (mean ± SEM; 4 mice) during the first day of training to 8.4 ± 0.3 s during the last day of training with a slope of 0.2 ± 0.05 s per day ($p = 0.04$) (Figs. 5d and S4d). The onset always occurred after the presentation of the reward at 8.0 s. In the absence of any reward, we observed a transient release of ACh when animals engaged in bouts of high frequency licking, similar to reward retrieval (15 events across 4 mice) (Fig. S4e). These findings suggest that ACh release may be involved in the motor behavior of licking following presentation of the reward (US). Interestingly, ACh release could not be detected by the M1-CNIiFERs during anticipatory licking, in contrast to DA release.

The extent of DA release correlates with anticipatory licking

Real-time measurements of neurotransmitter release revealed that the release of DA correlates with learning the association of CS with US while the release of NE appeared uncorrelated and that of ACh tracked the motor behavior associated with the US. We next

examined the shift in timing of DA release on a trial-by-trial basis for each mouse. Mice that exhibited a small change in the timing of DA release did not show significant anticipatory licking (Fig. 5e; **top**). By contrast, mice that demonstrated a strong shift in DA release also demonstrated a significant change in anticipatory licking (Fig. 5e; **bottom**). For all 13 mice, we compared the rate of change in DA release with the rate of change in anticipatory licking across all trials. We found that the rate of change in the release of DA strongly and significantly correlated with the rate of change in anticipatory licking (slope = 0.4 ± 0.1, SEM, p = 0.003) (Fig. 5f). There was no significant correlation between the highly variable release of NE (Fig. 5c) and the animal's licking behavior (p = 0.10). We conclude that DA release tracks the extent of learning as defined by changes in the licking behavior.

DISCUSSION

Here we report the creation of a new family of cell-based CNiFERs for rapid, optical detection of monoamine neurotransmitters released *in vivo*. Previously, CNiFERs were limited to GPCRs that coupled to G_q G-proteins[15]. Redirecting the $G_{i/o}$-coupled D2 receptor to the PLC/IP_3 pathway using a chimeric G-protein (G_{qi5}) was essential for developing the D2-CNiFER. It should now be possible to create CNiFERs for other G_i-coupled receptors, such as those for somatostatin, serotonin and opioids. The D2- and α1a-CNiFERs exhibit nanomolar sensitivity similar to their endogenous counterparts in neurons, have a temporal resolution of seconds, and exhibit a dynamic range suitable to discriminate between DA and NE *in vivo* (Fig. 2). The development of these CNiFERs offers significant advantages over current methods for detecting neurotransmitter release *in vivo*. While voltammetry techniques can measure DA and NE with fast temporal resolution and sensitivity and minimal damage to the cortex, they discriminate poorly between DA and NE as a result of their similar redox profiles[13]. Microdialysis can accurately distingiush DA and NE but lacks temporal resoution and requires physical implantation of a cannula, which itself can produce damage to the brain and disrupt monoaminergic activity near the probe track[12]. The D2- and α1a-CNiFERs can provide real-time optical measurements of both DA and NE release *in vivo* with relatively little impact on the brain.

The method described here to detect changes in the FRET ratio from multiple CNiFERs is ideal for imaging experiments with head-fixed mice. Implanting CNiFERs into subcortical structures and using a fiber[37,38] or GRIN lens/endoscope[39,40] to measure changes in FRET could be used to study neuromodulation in freely moving animals with implanted CNiFERs. Creating CNiFERs with different sensitivities could provide new information about the status of signaling through various second messenger pathways. For example, a DA-sensitive CNiFER for detecting higher concentrations of DA could be developed with the D1 dopamine receptor, which signals via the Gs pathway[41]. The methodology developed here to detect DA and NE could also be expanded to any neurotransmitter that signals through a GPCR and thus provides an important and versatile tool for neuroscientists that study circuit dynamics and brain states. While the CNiFERs may well be supplanted by the development of molecular indicators that are expressed on the surface of neurons or glia, such technologies are currently only available for the detection of glutamate[42,43] and are 100-fold less sensitive than CNiFERs (Fig. 1d). Moreover, these molecular detectors may also alter the physiology of the neuron or glia cell.

The ability of the D2-CNiFER and α1a-CNiFER to chemically discriminate NE from DA while retaining fast temporal resolution provides a unique opportunity to analyze the dynamics of neurotransmitter release on a trial-by-trial basis during learning (Fig. 4). The observed release of DA (Figs. 4 and 5) is consistent with previous studies that demonstrate that firing rates of DA neurons in basal ganglia increase in response to rewarding stimuli in both monkeys[44,45] and rodents[46,47]. The monotonic shift in DA release over five days of pairing the CS with the US (Fig. 5b) is consistent with the temporal difference model proposed by Schultz and colleagues[19,48], in which DA neurons respond to reward-predicting cues. Interestingly, the gradual shift in DA release contrasts with a previous study of midbrain DA neurons in which these neurons increased their firing rate either just after the reward or just after the cue[49]. Similarly, studies using FSCV demonstrated a shift in DA release from the US to CS in the NAc of rats[24,25]. One possible difference was that the 5 s period of the CS used in our study might have facilitated the observation of a more gradual shift of the response to the start of the cue. Alternatively, DA neurons that project to the cortex may have been underrepresented in our measurements, or the firing of DA neurons in the midbrain may not correlate with release of DA in the cortex, though these scenarios seem unlikely. Optogenetic control of DA neuronal activity showed that phasic firing enhances DA release in the striatum[2,50], though DA levels were not measured in the cortex.

While DA release appeared tightly correlated with the CS after training, NE release occurred during the trial but was highly variable between and within mice, exhibiting a very weak correlation with the CS or US as measured by the α1a-CNiFER (Fig. 5c). Other groups have shown that like DA neurons, LC neurons fire in tonic and burst modes, with LC phasic firing typically occurring following task cues (CS) but preceding lever responses (US)[3,4,20]. Acetylcholine release, on the other hand, correlated with the US and licking, but not with the CS. Thus, ACh and NE are both released during training trials but appear to respond to different cues. In conclusion, with the development of these new D2- and α1a-CNiFERs, along with the M1-CNiFER[15], it will be now possible to study the spatial and temporal resolution of multiple neurotransmitters released in more complex behavioral tasks.

ONLINE METHODS

Stably expressing cell lines

To create CNiFERs, a FRET-based Ca^{2+}-detector, TN-XXL, was first stably expressed in HEK293 cells transduced with replication deficient lentivirus as described previously[51]. In brief, cDNA for TN-XXL, GPCRs, and Gqi5 as needed was subcloned into the HIV-based cloning plasmid pCDH1-MCS1-EF1-Puro (System Biosciences) and lentiviral particles were produced by the UCSD Vector Development Laboratory (Atsushi Miyanohara, UCSD) or Salk GT[3] core. Clonal separation and selection were based on fluorescence intensity using flow cytometry (FACSaria, BD Biosciences), and response to internal calcium concentration increase in the presence of 3 μM ionomycin (Sigma).

For constructing specific receptor expressing clones, we used the human D2 receptor (NM_000795; UMR cDNA resource center) and the human α1a (AY389505, UMR cDNA resource center). After selection of a single clone, “TN-XXL only CNiFERs (3g8)” were transduced with lentivirus expressing the α1a adrenergic receptor. For the D2 receptor

CNiFER, 'TN-XXL only CNiFERs' were first transduced with lentivirus expressing the chimeric G_{qi5} protein, to enable coupling of the Gi-linked D2 receptor with the Gq-Ca^{2+} signaling pathway[16]. We identified the best qi5-expressing clone by transiently expressing the D2 receptor, and selecting a qi5 clone that gave the appropriate agonist response with the smallest background response. The qi5 clone was then transduced with a lentivirus that expressed the D2 receptor. Clonal separation and selection was based on fluorescence intensity using flow cytometry. Single α1a-CNiFER (α1a.6) and D2-CNiFER (D2.2) clones were ultimately selected based on their dose response curves to both dopamine and norepinephrine (Sigma). All CNiFER cells were maintained at 37°C with 5 % (v/v) CO_2. Upon confluence, cells were trypsinized, triturated, and seeded into new flasks using Dulbecco's Modification of Eagle's Medium (Cellgro®; Mediatech) with 10 % (v/v) of Fetalplex™ serum (Gemini Bio-Products), 100 U/ml of penicillin and 100 μg/ml of streptavidin (Gibco). Control-CNiFERs with only the TN-XXL calcium indicator (3g8) or with TN-XXL calcium indicator and the chimeric G_{qi5} protein (qi5.6) were maintained in the same conditions.

In vitro high-throughput testing

D2- and α1a-CNiFER FRET responses to different neurotransmitters were measured *in vitro* using a high-throughput fluorometric plate reader (FlexStation3, Molecular Devices). The day before experiments, CNiFERs were plated on fibronectin-coated 96-wells plates. Thirty minutes before experiments, media in each well was replaced with 100 μl artificial cerebral spinal fluid (ACSF; 125 mM NaCl, 5 mM KCl, 10 mM D-glucose, 10 mM HEPES, 3.1 mM $CaCl_2$, 1.3 mM $MgCl_2$, pH 7.4) and plates were loaded into the FlexStation3. Experiments were conducted at 37°C using 436 nm excitation light. Light was collected at 485 ± 10 nm for CFP (eCFP) and 527 ± 12 nm for YFP (Citrine) every 3.8 s. After 30 s of baseline, 50 μl of drug diluted in ACSF was delivered to each well. Background measurements taken from wells without cells were subtracted, fluorescence intensities were normalized to pre-stimulus baselines, and peak responses were measured from the ratio of the 527 nm and 485 nm channels.

In vitro characterization

D2- and α1a-CNiFERs were trypsinized and plated on fibronectin-coated coverslips. The following day, CNiFERs were placed in a cell culture chamber (RC26; Warner Instruments) and perfused with gravity-fed ACSF. Chamber fluid temperature was kept at 35°C by a temperature controller (TC-324B; Warner Instruments). To test the receptor specificity of the D2-CNiFER, FRET responses were measured during two 60 s presentations of 20 nM dopamine. The second presentation was preceded by 60 s of either 100 nM D1-receptor antagonist, SCH23390 (Tocris), or 50 nM D2-receptor antagonist, eticlopride (Tocris). Percent response remaining was calculated by subtracting the peak FRET response during the second DA presentation (in the presence of antagonist) from the first (in the absence of antagonist). α1a-CNiFER receptor specificity was similarly tested using two 60 s presentations of 50nM norepinephrine with the second presentation being preceded by 180 s of either 5 μM β-adrenergic receptor antagonist, sotatol (Tocris), or 50 μM α1a-acceptor antagonist, WB4101 (Tocris). For repeat pulse experiments, D2- and α1a-CNiFERs were given 10 presentations of either 60 s 50 nM dopamine or 500 nM norepinephrine,

respectively, followed by 180 s of ACSF alone. For temporal discrimination experiments, cells were imaged with a two-photon microscope (see next section), and rapid drug presentation was achieved with a fast perfusion stepper (SF-77B; Warner Instruments). The agonist was mixed with Alexa-594 in the drug pipette to determine perfusion time. The Alexa 594 signal was imaged simultaneously with the CNiFER FRET response on a third channel.

TPLSM imaging

CNiFER cells were imaged with a custom-built two-photon laser-scanning microscope. Control of scanning and data acquisition was achieved through the MPScope software suite[52]. Excitation light at 820 nm was used to excite the CFP portion of TN-XXL. Fluorescence was collected by either a 25X water objective (HCX-IRAPO, Leica) for *in vivo* experiments or a 10X air objective (PLAN-NEOFLUAR, Zeiss) for *in vitro* experiments. The fluorescent signal was split into two or three channels: 470 ± 20 nm for measurement of emission by CFP, 535 ± 20 nm for emission by YFP (Citrine), and 620 ± 20 nm for emission by Alexa 594

Animal preparation

Adult, female C57BL/6 mice, age P60 to P90, were maintained in standard cages on a natural light-dark cycle. The Institutional Animal Care and Use Committee at the University of California San Diego approved all protocols. For surgery, mice were anesthetized with isoflurane (Butler Schein). Body temperature was monitored and maintained at 37°C. Subcutaneous injections of 5 % (w/v) glucose in saline were given every 2 h for rehydration. Buprenorphine (0.02 mg/kg, Butler Schein) was administered i.p. for post-operative analgesia.

Retrograde labeling

After anesthesia, mice were placed in a stereotaxic frame. A small craniotomy was performed where CNiFERs were typically injected (+1.5 mm A/P, +1.5 mm M/L). Using a 10 μm inner-diameter glass pipette connected to a Nanoinjector II (Drummond), 200 nl of Fluorogold™ (Fluorochrome), prepared as 1 % (w/v) in 0.1 M cacodylate buffer, was injected (20 nl every minute) in the cortex 200 μm from the surface. After 7 d, the mice were transcardially perfused. Histological sections were scanned at 1 μm spatial resolution using a Nanozoomer (Hamamatsu) digital slide scanner. Using Neurolucida software (Microbrightfield™), outlines of midbrain, brainstem, and cerebellum were drawn and sections were aligned based on anatomical borders to yield three-dimensional reconstructions. Outlines of subsantia nigra, ventral tegmental area and locus coeruleus were defined by tyrosine hydroxylase labeled neurons. Cells double-labeled for tyrosine hydroxylase and Fluorogold™ were marked and counted. Co-labeling was confirmed by confocal microscopy.

Histology

Mice were perfused with phosphate buffered saline (PBS), immediately followed by 4 % (w/v) paraformaldehyde (PFA) in PBS. Brains were post-fixed overnight at 4°C followed by

immersion in 30 % (w/v) sucrose. Brain sections, 30 or 50–μm thick, were cut using a sliding microtome. Primary antibodies (mouse anti-tyrosine hydroxylase, 1:1000, Millipore; rabbit anti-Fluorogold™, 1:5000, Millipore; mouse anti-GFAP, 1:1000, Millipore; rat anti-MAC1, 1:500, Millipore) were diluted in a buffer that consisted of 10 % (v/v) goat serum (Vector Labs) and 0.1 % (v/v) Triton X-100. Free-floating sections were then incubated overnight under slow rotation at 20°C in primary antibody solution, washed 3-times with PBS and incubated with secondary antibody (Alexa 488 anti-mouse, Alexa 594 anti-mouse, Alexa 594 anti-rat, and Alexa 594 anti-rabbit, 1:2000, Molecular Probes) for 2 h. Sections were then washed and incubated 15 minutes in NeuroTrace® Blue (Life Technologies), a Nissl stain for visualizing neuron. Sections were washed again and mounted with Fluoromount™-G (Southern Biotechnology Associates).

CNiFER implantation

CNiFERs were harvested without trypsin from 80 % confluent culture flasks, centrifuged, and re-suspended in ACSF for injection. For the *in vivo* dose response experiment, a open craniotomy was used. For all other *in vivo* experiments, a 'thinned skull' craniotomy[34] was used. CNiFER cells were loaded into a 40 μm inner-diameter glass pipette connected to a Nanoinjector II (Drummond) and injected into neocortex through the thinned skull ~200 μm from the cortical surface. CNiFERs were injected into adjacent sites within the following stereotaxic coordinates: +1 to +2 mm A/P; +1 to +2 mm M/L. After implantation in several adjacent sites (typically two injection sites per CNiFER variant), the craniotomy was sealed with a glass coverslip. A custom-built head-bar was attached to the skull with C&B-METABOND (Parkell, Inc.), and the preparation surrounding the imaging window was covered with dental cement (Dentsply). Mice were immunosuppressed by daily cyclosporine injection (20 μl/100 g, i.p., Belford Laboratories).

Electrical stimulation and *in vivo* pharmacology

Mice were prepared and injected with CNiFERs as described. Additionally, a 0.1 MΩ tungsten bipolar stimulating electrodes with a tip separation of 500 μm (Microprobes Inc.) was implanted into either substantia nigra (−3.2 mm A/P, −1.3 mm M/L, −4.4 mm D/V) or locus coeruleus (−5.3 mm A/P, −0.9 mm M/L, −3.4 mm D/V). After a day of recovery, imaging was performed under isoflurane anesthesia. Experimental runs consisted of 30s baseline followed by electrical stimulation (200 μs pulses of 50 – 300 μA at 50 Hz for 500 ms). To test the specificity of the response, eticlopride (1mg/kg, Sigma), WB4101 (2 mg/kg, Tocris), or cocaine (15mg/kg; Sigma) were injected i.p. 10 minutes before the electrical stimulation.

In vivo dose response

After CNiFER implantation, the craniotomy was kept open and a glass pipette connected to a Nanoinjector II (Drummond) was positioned, using a Sutter manipulator, 100 μm away from the CNiFER implants. Imaging was performed under urethane anesthesia (1.5g/Kg, IP). The agonist, *i.e.*, NE or DA, was mixed with Alexa 594 to verify the arrival of the agonist as well as the calculate dilution of the agonist between the pipet and the implant. A long train of pulses of agonist (2.3 nl pressure injections as 2 s pulses every 5 s until a steady

state response was observed, typically after 30 s) was then applied next to the CNiFER implants. Control pulses of Alexa 594 in saline did not cause any FRET change. The dilution was calculated by measuring the average fluorescence of the Alexa 594 in the interstitial space of the implant and comparing it to the average fluorescence of the dye in the void immediately downstream from the pipette.

In vivo awake imaging and behavior

After one day of recovery from surgery, mice were water deprived (23 h/day). Conditioning started the following day. Animals were placed in a stationary head-frame and imaged while being presented with a 5 s tone (CS), followed by a 3 s delay and a drop of 10 % (w/v) sucrose-water (US), with an average inter-trial interval of three minutes. Two CNiFER variants, *i.e.*, α1a- and D2-CNiFERs or M1- and D2-CNiFERs, were imaged simultaneously. Licking behavior was recorded using a custom-built, conductance-based sensor. Mice were imaged for 10 to 15 trials and then returned to their home cage. Animals were imaged once a day for 5 consecutive days.

Data analysis

All the TPLSM data analysis was done using Matlab (MathWorks). TN-XXL fluorescence intensities were background-subtracted and normalized to pre-stimulus baselines. Regions of interest were drawn around either the D2- or the α1a-CNiFER implants. Responses were quantified as the fractional change in the FRET ratio ΔR/R, where ΔR is the change in the ratio of fluorescence intensities of the two channels, denoted $F_{530\ nm}$ and $F_{475\ nm}$, respectively, and R is the normalized baseline ratio, such that:

$$\frac{\Delta R(t)}{R} \equiv \frac{F_{530\,nm}(t)}{\langle F^{baseline}_{530\,nm}\rangle_{prestim}} \Big/ \frac{F_{475\,nm}(t)}{\langle F^{baseline}_{475\,nm}\rangle_{prestim}} - 1$$

Responses were measured at the peak of ΔR/R after low-pass filtering. For *in vitro* high-throughput testing, the peak responses were determined using Matlab, and the EC_{50} and Hill coefficient were calculated using Prism software (GraphPad). For behavioral experiments, the onset of the FRET signal was analyzed using Matlab. The onset of the FRET signal was defined as the point at which the ratio ΔR/R increased by 2.5-times the root-mean-square level of the baseline noise, typically ΔR/R ~ 0.03. Each onset time was scored manually by two experimenters that were blind to the time of the CS and the US. Only trials in which animals responded after CS presentation and within 30 s of US presentation were used for analysis. Statistical analyses were calculated using Prism software (GraphPad).

Supplementary Material

Refer to Web version on PubMed Central for supplementary material.

Acknowledgments

We thank Bruce Conklin for providing the Gqi5 cDNA, Allan Schweitzer for assistance with the electronics, Natalie Taylor for assistance with screening of clones, Takaki Komiyama and Wolfram Schultz for discussions, and the reviewers for excellent suggestions. This work was supported by research grants through NIDA (DA029706),

NIBIB (EB003832), and Hoffman-La Roche (88610A) and by the “Neuroscience Related to Drugs of Abuse” training grant through NIDA.

References

1. Adamantidis AR, Tsai HC, Boutrel B, Zhang F, Stuber GD, Budygin EA, Tourino C, Bonci A, Deisseroth K, de Lecea L. Optogenetic interrogation of dopaminergic modulation of the multiple phases of reward-seeking behavior. Journal of Neuroscience. 2011; 31:10829–10835. [PubMed: 21795535]
2. Tsai HC, Zhang F, Adamantidis A, Stuber GD, Bonci A, de Lecea L, Deisseroth K. Phasic firing in dopaminergic neurons is sufficient for behavioral conditioning. Science. 2009; 324:1080–1084. [PubMed: 19389999]
3. Aston-Jones G, Cohen JD. Adaptive gain and the role of the locus coeruleus-norepinephrine system in optimal performance. Journal of Comparative Neurology. 2005; 493:99–110. [PubMed: 16254995]
4. Bouret S, Sara SJ. Network reset: A simplified overarching theory of locus coeruleus noradrenaline function. Trends in Neuroscience. 2005; 28:574–582.
5. Floresco SB. Prefrontal dopamine and behavioral flexibility: Shifting from an “inverted-U” toward a family of functions. Frontiers of Neuroscience. 2013; 7:e62.
6. Edeline JM, Manunta Y, Hennevin E. Induction of selective plasticity in the frequency tuning of auditory cortex and auditory thalamus neurons by locus coeruleus stimulation. Hearing Research. 2011; 274:75–84. [PubMed: 20709165]
7. Bao S, Chan VT, Merzenich MM. Cortical remodelling induced by activity of ventral tegmental dopamine neurons. Nature. 2001; 412:79–83. [PubMed: 11452310]
8. Day JC, Kornecook TJ, Quirion R. Application of *in vivo* microdialysis to the study of cholinergic systems. Methods. 2001; 23:21–39. [PubMed: 11162147]
9. Greco S, Danysz W, Zivkovic A, Gross R, Stark H. Microdialysate analysis of monoamine neurotransmitters: A versatile and sensitive LC-MS/MS method. Analytica Chimica Acta. 2013; 771:65–72. [PubMed: 23522114]
10. Ji C, Li W, Ren XD, El-Kattan AF, Kozak R, Fountain S, Lepsy C. Diethylation labeling combined with UPLC/MS/MS for simultaneous determination of a panel of monoamine neurotransmitters in rat prefrontal cortex microdialysates. Analytical Chemistry. 2008; 80:9195–9203. [PubMed: 19551941]
11. Mingote S, de Bruin JPC, Feenstra MG. Noradrenaline and dopamine efflux in the prefrontal cortex in relation to appetitive classical conditioning. Journal of Neuroscience. 2004; 24:2475–2480. [PubMed: 15014123]
12. Wang Y, Michael AC. Microdialysis probes alter presynaptic regulation of dopamine terminals in rat striatum. Journal of Neuroscience Methods. 2012; 208:34–39. [PubMed: 22546476]
13. Robinson DL, Venton BJ, Heien ML, Wightman RM. Detecting subsecond dopamine release with fast-scan cyclic voltammetry in vivo. Clinical Chemistry. 2003; 49:1763–1773. [PubMed: 14500617]
14. Park J, Takmakov P, Wightman RM. In vivo comparison of norepinephrine and dopamine release in rat brain by simultaneous measurements with fast-scan cyclic voltammetry. Journal of Neurochemistry. 2011; 119:932–944. [PubMed: 21933188]
15. Nguyen QT, Schroeder LF, Mank M, Muller A, Taylor PW, Griesbeck O, Kleinfeld D. An *in vivo* biosensor for neurotransmitter release and *in situ* receptor activity. Nature Neuroscience. 2010; 13:127–132. [PubMed: 20010818]
16. Conklin BR, Farfel Z, Lustig KD, Julius D, Bourne HR. Substitution of three amino acids switches receptor specificity of Gq alpha to that of Gi alpha. Nature. 1993; 363:274–276. [PubMed: 8387644]
17. Schultz W. Updating dopamine reward signals. Current Opinion in Neurobiology. 2013; 23:229–238. [PubMed: 23267662]

18. Feenstra MG. Dopamine and noradrenaline release in the prefrontal cortex in relation to unconditioned and conditioned stress and reward. Progress in Brain Research. 2000; 126:133–163. [PubMed: 11105645]
19. Schultz W, Dayan P, Montague PR. A neural substrate of prediction and reward. Science. 1997; 275:1593–1599. [PubMed: 9054347]
20. Bouret S, Richmond BJ. Relation of locus coeruleus neurons in monkeys to Pavlovian and operant behaviors. Journal of Neurophysiology. 2009; 101:898–911. [PubMed: 19091919]
21. Yamauchi JG, Nemecz A, Nguyen QT, Muller A, Schroeder LF, Talley TT, Lindstrom J, Kleinfeld D, Taylor P. Characterizing ligand-gated ion channel receptors with genetically encoded Ca^{2+} sensors. Public Library of Science ONE. 2011; 6:e16519. [PubMed: 21305050]
22. Engelman EA, Ingraham CM, McBride WJ, Lumeng L, Murphy JM. Extracellular dopamine levels are lower in the medial prefrontal cortex of alcohol-preferring rats compared to Wistar rats. Alcohol. 2006; 38:5–12. [PubMed: 16762687]
23. Ihalainen JA, Riekkinen P Jr, Feenstra GP. Comparison of dopamine and noradrenaline release in mouse prefrontal cortex, striatum and hippocampus using microdialysis. Neuroscience Letters. 1999; 277:71–74. [PubMed: 10624812]
24. Clark JJ, Sandberg SG, Wanat MJ, Gan JO, Horne EA, Hart AS, Akers CA, Parker JG, Willuhn I, Martinez V, Evans SB, Stella N, Phillips PEM. Chronic microsensors for longitudinal, subsecond dopamine detection in behaving animals. Nature Methods. 2010; 7:126–129. [PubMed: 20037591]
25. Day JJ, Roitman MF, Wightman M, Carelli RM. Associative learning mediates dynamic shifts indopamine signaling in the nucleus accumbens. Nature Neuroscience. 2007; 10:1020–1028. [PubMed: 17603481]
26. Hoffmann C, Gaietta G, Bunemann M, Adams SR, Oberdorff-Maass S, Behr B, Vilardaga JP, Tsien RY, Ellisman MH, Lohse MJ. A FlAsH-based FRET approach to determine G protein-coupled receptor activation in living cells. Nature Methods. 2005; 2:171–176. [PubMed: 15782185]
27. Falkenburger BH, Jensen JB, Hille B. Kinetics of M1 muscarinic receptor and G protein signaling to phospholipase C in living cells. Journal of General Physiology. 2010; 135:81–97. [PubMed: 20100890]
28. Loughlin SE, Fallon JH. Substantia nigra and ventral tegmental area projections to cortex: Topography and collateralization. Neuroscience. 1984; 11:425–435. [PubMed: 6201780]
29. Hoover JE, Strick PL. The organization of cerebellar and basal ganglia outputs to primary motor cortex as revealed by retrograde transneuronal transport of herpes simplex virus type 1. Journal of Neuroscience. 1999; 19:1446–1463. [PubMed: 9952421]
30. Middleton FA, Strick PL. Basal-ganglia ‘projections’ to the prefrontal cortex of the primate. Cerebral Cortex. 2002; 12:926–935. [PubMed: 12183392]
31. Hosp JA, Pekanovic A, Rioult-Pedotti MS, Luft AR. Dopaminergic projections from midbrain to primary motor cortex mediate motor skill learning. Journal of Neuroscience. 2011; 31:2481–2487. [PubMed: 21325515]
32. Gatter KC, Powell TP. The projection of the locus coeruleus upon the neocortex in the macaque monkey. Neuroscience. 1977; 2:441–445. [PubMed: 408733]
33. Loughlin SE, Foote SL, Bloom FE. Efferent projections of nucleus locus coeruleus: topographic organization of cells of origin demonstrated by three-dimensional reconstruction. Neuroscience. 1986; 18:291–306. [PubMed: 3736860]
34. Drew PJ, Shih AY, Driscoll JD, Knutsen PM, Davalos D, Blinder P, Akassoglou K, Tsai PS, Kleinfeld D. Chronic optical access through a polished and reinforced thinned skull. Nature Methods. 2010; 7:981–984. [PubMed: 20966916]
35. Zheng JQ, Felder M, Connor JA, Poo M-m. Turning of growth cones induced by neurotransmitters. Nature. 1994; 368
36. Berg RW, Friedman B, Schroeder LF, Kleinfeld D. Activation of nucleus basalis facilitates cortical control of a brainstem motor program. Journal of Neurophysiology. 2005; 94:699–711. [PubMed: 15728764]

37. Schulz K, Sydekum E, Krueppel R, Engelbrecht CJ, Schlegel F, Schröter A, Rudin M, Helmchen F. Simultaneous BOLD fMRI and fiber-optic calcium recording in rat neocortex. Nature Methods. 2012; 9:597–602. [PubMed: 22561989]
38. Stroh A, Adelsberger H, Groh A, Rühlmann C, Fischer S, Schierloh A, Deisseroth K, Konnerth A. Making waves: Initiation and propagation of corticothalamic Ca^{2+} waves *in vivo*. Neuron. 2013; 77:1136–1150. [PubMed: 23522048]
39. Levene MJ, Dombeck DA, Kasischke KA, Molloy RP, Webb WW. *In vivo* multiphoton microscopy of deep brain tissue. Journal of Neurophysiology. 2004; 91:1908–1912. [PubMed: 14668300]
40. Jung JC, Mehta AD, Aksay E, Stepnoski R, Schnitzer MJ. *In vivo* mammalian brain imaging using one- and two-photon fluorescence microendoscopy. Journal of Neurophysiology. 2004; 92:3121–3133. [PubMed: 15128753]
41. Robinson, DL.; Wightman, RM. Rapid dopamine release in freely moving rats. CRC Press; 2007.
42. Okubo Y, Sekiya H, Namiki S, Sakamoto H, Iinuma S, Yamasaki M, Watanabe M, Hirose K, Iino M. Imaging extrasynaptic glutamate dynamics in the brain. Proceedings of the National Academy of Sciences USA. 2010; 107:6526–6531.
43. Marvin JS, Borghuis BG, Tian L, Cichon J, Harnett MT, Akerboom J, Gordus A, Renninger SL, Chen TW, Bargmann CI, Orger MB, Schreiter ER, Demb JB, Gan WB, Hires SA, Looger LL. An optimized fluorescent probe for visualizing glutamate neurotransmission. Nature Methods. 2013; 10:162–170. [PubMed: 23314171]
44. Romo R, Schultz W. Dopamine neurons of the monkey midbrain: Contingencies of responses to active touch during self-initiated arm movements. Journal of Neurophysiology. 1990; 63:592–606. [PubMed: 2329363]
45. Schultz W, Apicella P, Ljungberg T. Responses of monkey dopamine neurons to reward and conditioned stimuli during successive steps of learning a delayed response task. Journal of Neuroscience. 1993; 13:900–913. [PubMed: 8441015]
46. Kosobud AE, Harris GC, Chapin JK. Behavioral associations of neuronal activity in the ventral tegmental area of the rat. Journal of Neuroscience. 1994; 14:7117–7129. [PubMed: 7965102]
47. Miller JD, Sanghera MK, German DC. Mesencephalic dopaminergic unit activity in the behaviorally conditioned rat. Life Sciences. 1981; 29:1255–1263. [PubMed: 7300554]
48. Montague PR, Dayan P, Sejnowski TJ. A framework for mesencephalic dopamine systems based on predictive Hebbian learning. Journal of Neuroscience. 1996; 16:1936–1947. [PubMed: 8774460]
49. Pan WX, Schmidt R, Wickens JR, Hyland BI. Dopamine cells respond to predicted events during classical conditioning: Evidence for eligibility traces in the reward-learning network. Journal of Neuroscience. 2005; 25:6235–6242. [PubMed: 15987953]
50. Gradinaru V, Mogri M, Thompson KR, Henderson JM, Deisseroth K. Optical deconstruction of Parkinsonian neural circuitry. Science. 2009; 324:354–359. [PubMed: 19299587]
51. Mank M, FSA, Direnberger S, Mrsic-Flogel TD, Hofer SB, Stein V, Hendel T, Reiff DF, Levelt C, Borst A, Bonhoeffer T, Hübener M, Griesbeck O. A genetically encoded calcium indicator for chronic *in vivo* two-photon imaging. Nature Methods. 2008; 5:805–811. [PubMed: 19160515]
52. Nguyen, Q-T.; Dolnick, EM.; Driscoll, J.; Kleinfeld, D. Methods for In Vivo Optical Imaging. 2. Frostig, RD., editor. CRC Press; 2009. p. 117-142.

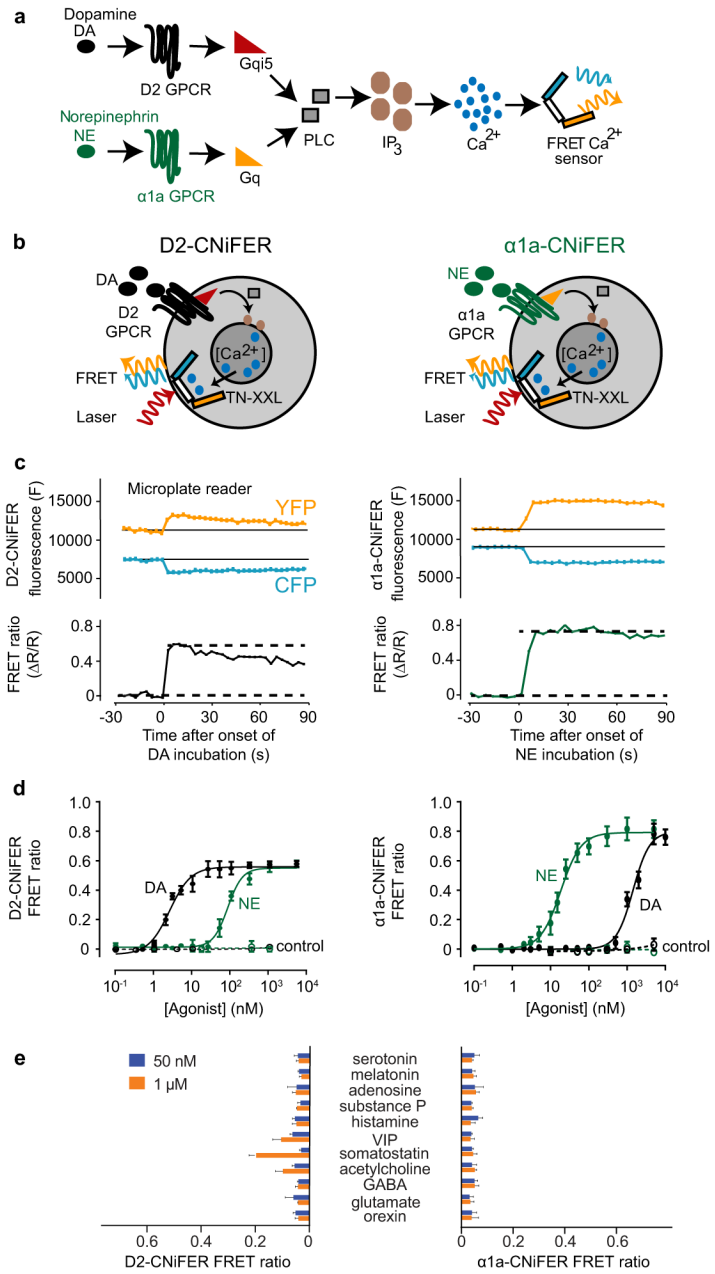

Figure 1. Design of D2- and α1a-CNiFERs and their *in vitro* characterization using a high-throughput plate reader

(a) Schematic of CNiFER signaling pathway. Dopamine (DA) stimulation of D2 GPCR leads to activation of G_{qi5} chimeric proteins. Norepinephrine (NE) stimulation of α1a GPCR leads to activation of G_q G-proteins. Activated G_q stimulates phospholipase C (PLC), producing signaling intermediate inositol triphosphate (IP_3) which stimulates release of Ca^{2+}, detected by the FRET based TN-XXL calcium sensor. **(b)** Depiction of DA activating D2 receptor (left, black) and NE activating α1a receptor (right, green) to induce IP_3-mediated Ca^{2+} cytoplasmic influx detected by TN-XXL. Fluorescence from laser-excited enhanced cyan fluorescent proteins and citrine fluorescent proteins flanking TN-XXL is

collected for the FRET signal. **(c)** FRET response of D2-CNiFER to continuous application of 100 nM DA (left) and α1a-CNiFER to continuous application of 100 nM NE (right). Example of transmitter-induced concurrent, opposing responses in citrine (530 nm) and cyan (475 nm) fluorescence (top) represented as a FRET ratio (bottom). **(d)** Left**,** Dose response curves for D2-CNiFER and control CNiFERs with only calcium indicator and chimeric G_{qi5} protein (dashed line) in response to DA (black) or NE (green) (n = 3). Right, Dose response curves for α1a-CNiFER and control CNiFERs with only calcium indicator (dashed line) in response to DA (black) or NE (green)(n=3). Error bars represent standard deviation. **(e)** Summary of D2-CNiFER (left) and α1a-CNiFER (right) FRET responses to a panel of neurotransmitters at 50 nM and 1 μM. VIP, vasoactive intestinal peptide; GABA, gamma-aminobutyric acid. Error bars represent standard deviation (n = 3).

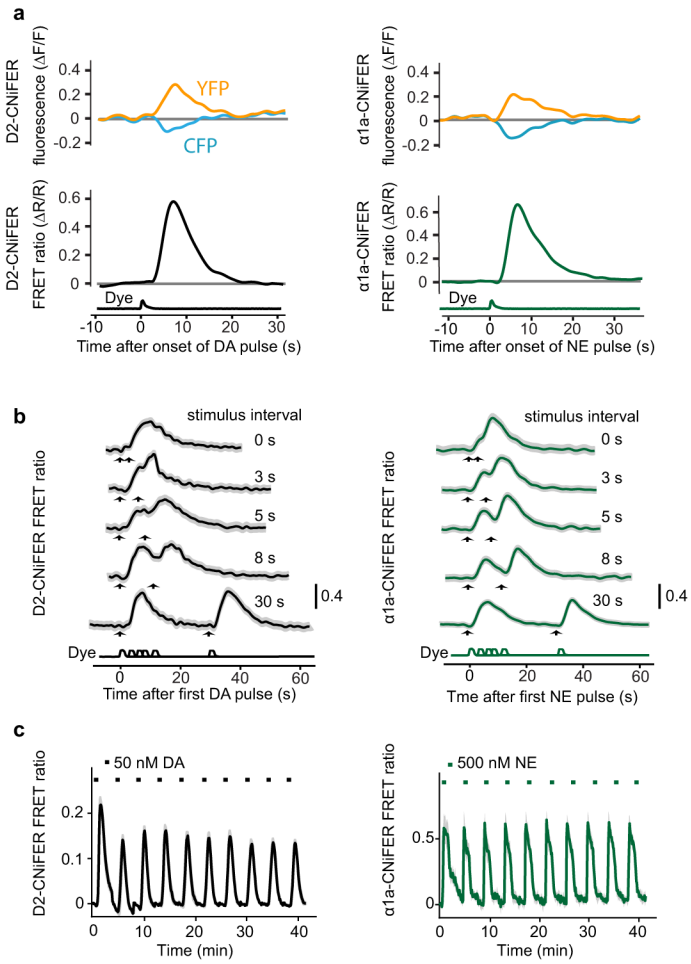

Figure 2. *In vitro* characterization of CNiFERs to a pulse or pulses of agonist

(a) Single-trial FRET response of a cluster of approximately fifty D2-CNiFERs to 2.5 s pulse of 100 nM DA (left) and a cluster of approximately fifty α1a-CNiFERs to a 2.5 s pulse of 100nM NE (right). Top traces, examples of transmitter-induced FRET responses for D2 CNiFER (left) and α1a CNiFER (right); note opposing responses in citrine (530 nm) and cyan (475 nm) fluorescence. Middle traces show calculated FRET ratio (ΔR/R). Bottom traces show Alex-594 fluorescence to monitor time course of agonist pulse. **(b)** Left, temporal discrimination of D2-CNiFER FRET responses to delivery of two 2.5 s pulses of 100 nM DA with variable interstimulus intervals (n = 3). Right, discrimination of α1a-CNiFER responses to two pulses of 100 nM NE (n = 3). Shaded grey areas represent standard error. **(c)** D2-CNiFER (left) and α1a-CNiFER (right) FRET responses to repeated 60 s pulses of 50 nM DA (black dashes, n = 3) or 500 nM NE (green dashes, n = 3.) followed by 180 s of ACSF. Shaded areas are standard error.

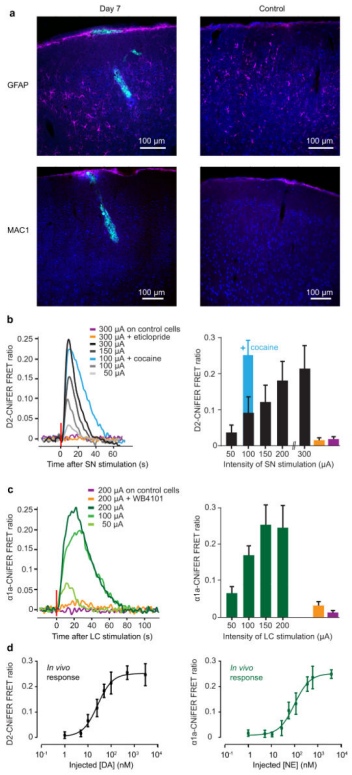

Figure 3. ***In vivo*** **characterization of D2- and α1a-CNiFERs**

(a) Immunostaining for GFAP (magenta, top panel), MAC1 (magenta, lower panel) and NeuroTrace® (blue), in coronal sections. Left, mouse perfused 7 d after the injection of CNiFERs (green) in the frontal cortex. Right, control mouse with a similar optical window but no CNiFER injection. **(b)** D2-CNiFER FRET responses (evoked in frontal cortex by increasing amplitude of SN electrical stimulation before (black and grey, n = 4) and after i.p. injection of D2-receptor antagonist eticlopride (1mg/kg, orange, n = 3) or the DA reuptake inhibitor cocaine (15 mg/kg, blue, n = 3). Purple, response of control CNiFER to high amplitude stimulation. Left, example of raw traces used to calculate average peak responses (right) for each stimulation intensity. **(c)** α1a-CNiFER FRET response (green, n = 3) evoked by LC stimulation before (green) and after i.p. injection of α1a-receptor antagonist WB4101 (2mg/kg, orange, n = 3). Purple, response of control CNiFER to high amplitude stimulation. Example traces (left) and average peak responses (right). Error bars represent standard deviation. **(d)** Left, *in vivo* dose response curve for D2-CNiFER (black, n = 4). Right, *in vivo* dose response curve for α1a-CNiFER (green, n = 4). Error bars represent standard deviation.

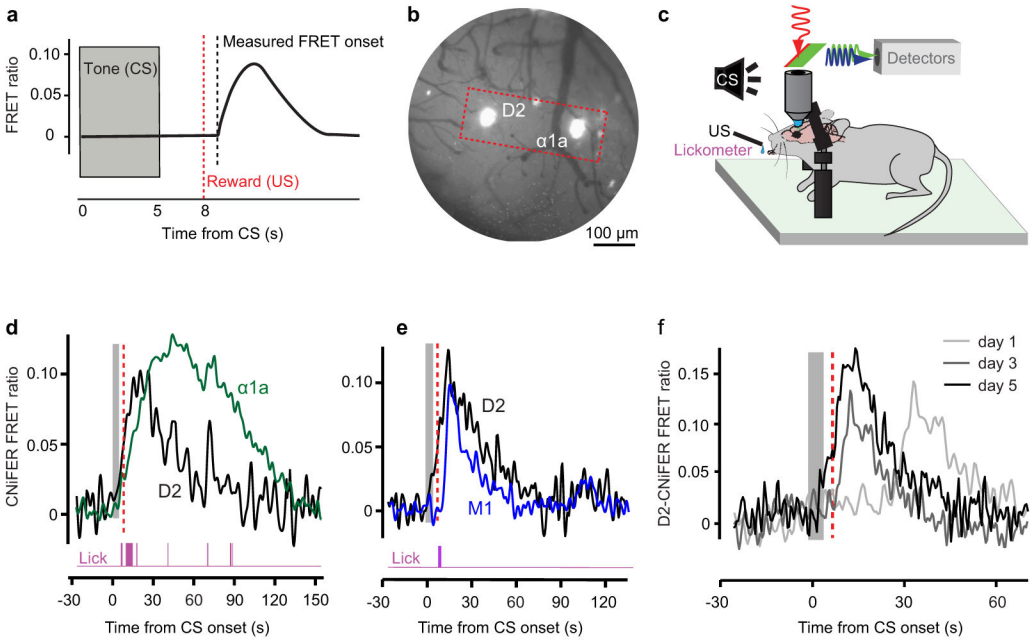

Figure 4. Simultaneous detection of DA, NE, and ACh release during behavioral conditioning

(a) Schematic of CNiFER FRET response and onset time measurement during a single conditioning trial. Conditioning trials consisted of a 5 s tone (conditioning stimulus, CS, grey) followed by a 3 s delay and delivery of a drop of 10 % (w/v) sucrose water (unconditioned stimulus, US, red). **(b)** Brightfield image of the surface vasculature superimposed with fluorescent picture of the CNiFERs. D2-CNiFERs and α1a-CNiFERs implanted next to each other into frontal cortex. The red box shows the field of view that was used to image both CNiFERs simultaneously. **(c)** Procedure to measure licking behavior and CNIFER fluorescence in head-restrained mice during classical conditioning. **(d)** Simultaneous measurement of D2- (black) and α1a-CNiFER (green) FRET responses and licking (purple) during a single conditioning trial. **(e)** Simultaneous measurement of D2- (black) and M1-CNiFER (blue) FRET responses and licking (magenta) during a single conditioning trial. (**f**) Single trace examples of the D2-CNiFER response in the same animal at day 1, 3 and 5 of training.

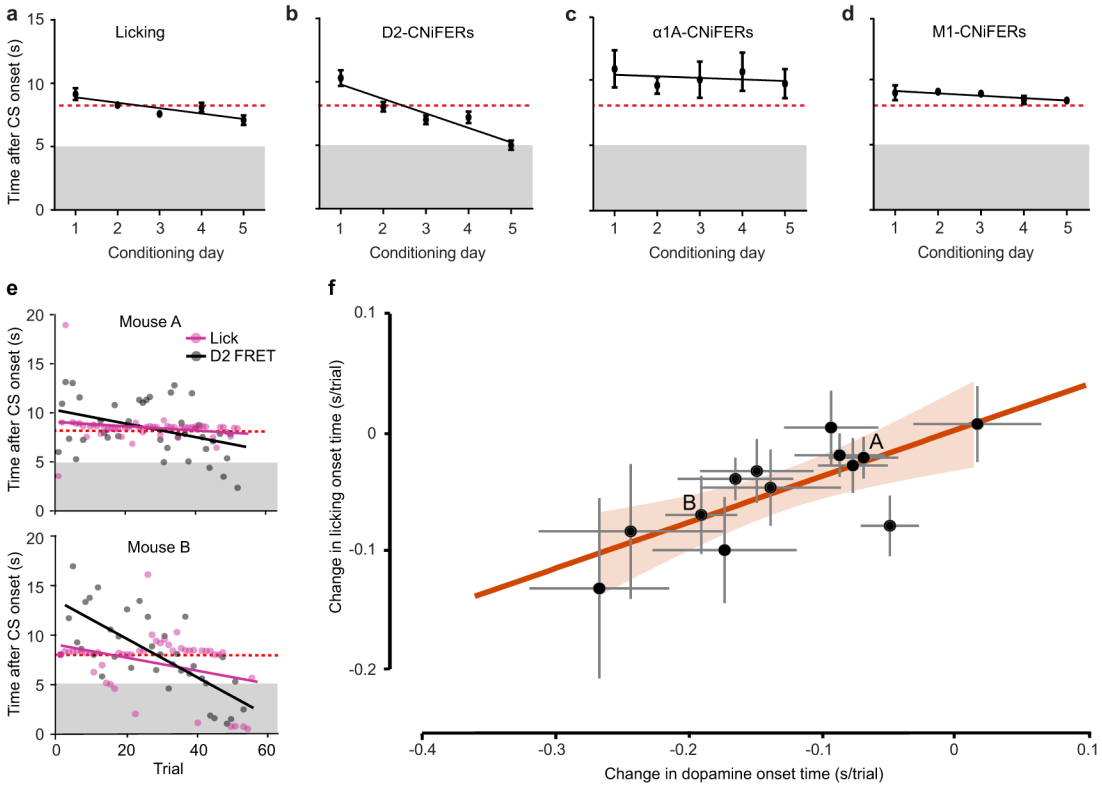

Figure 5. Shift in DA but not NE release with behavioral conditioning

(a–d). Population averages of response onset times per day of conditioning. Error bars represent standard error. (**a)** Licking onset times during conditioning trials (CS, grey bar; US, dashed red line) across five days of conditioning (n = 13). **(b)** D2-CNiFER FRET response onset times during conditioning. FRET onset times are measured relative to CS onset (n = 13) **(c)** α1a-CNIFER onset times during conditioning (n = 7). **(d)** M1-CNiFER onset times during conditioning. **(e)** Onset time of D2-CNiFER FRET response (black) and licking (magenta) across conditioning trials for two mice A and B. Solid lines, best fit linear regressions of CNiFER responses and licking. Grey area, time of CS presentation; dashed red line, time of US presentation. (**f)** Correlation between rate of change in DA onset and rate of change in licking onset across conditioning trials. Each point represents the rate relationship for one animal with standard deviation (grey error bars). Orange line, linear regression with 95 % confidence intervals (orange shaded area, n = 13).